23. Conditions for metathesis reaction: **1a** or **2a**, prepared from the corresponding diazoalkanes, was immersed in a solution (0.1 M solution in THF) of the corresponding alkenes for 2 hours. The films were removed, rinsed with fresh THF, and dried under a stream of nitrogen gas.
24. The generalized gradient approximation was used (*12*, *25*).
25. J. P. Perdew, K. Burke, M. Ernzerhof, *Phys. Rev. Lett.* **77**, 3865 (1996).
26. Jaguar 5.0, Schrodinger, L.L.C., Portland, OR (1991–2003).
27. The ABINIT code is a common project of the Université Catholique de Louvain, Corning Incorporated, and other contributors (www.abinit.org).
28. X. Gonze *et al.*, *Comp. Mater. Sci.* **25**, 478 (2002).
29. The substructure of the occupied resonance is due to the size of the slab (4 monolayers). However, there is continuous state density through this energy region, resulting from dispersion of the states in the direction parallel to the surface.
30. We acknowledge primary financial support from the Nanoscale Science and Engineering Initiative of the NSF under NSF award number CHE-0117752 and by the New York State Office of Science, Technology, and Academic Research (NYSTAR). We acknowledge support from the Chemical Sciences, Geosciences and Biosciences Division, Office of Basic Energy Sciences, U.S. Department of Energy (#DE-FG02-01ER15264). C.N. thanks the American Chemical Society Petroleum Research Fund type G (#39263-G7), the Camille Dreyfus Teacher Scholar Program (2004), and the Alfred P. Sloan Fellowship Program (2004). We thank the Materials Research Science and Engineering Center Program of the NSF under award number DMR-0213574 and by the NYSTAR for financial support for M.L.S. and the shared instrument facility.

Supporting Online Material
www.sciencemag.org/cgi/content/full/309/5734/591/DC1
Materials and Methods
Figs. S1 to S5
Table S1
References

25 March 2005; accepted 10 June 2005
10.1126/science.1112767

Martian Surface Paleotemperatures from Thermochronology of Meteorites

David L. Shuster[1]* and Benjamin P. Weiss[2]†

The temporal evolution of past martian surface temperatures is poorly known. We used thermochronology and published noble gas and petrographic data to constrain the temperature histories of the nakhlites and martian meteorite ALH84001. We found that the nakhlites have not been heated to more than 350°C since they formed. Our calculations also suggest that for most of the past 4 billion years, ambient near-surface temperatures on Mars are unlikely to have been much higher than the present cold (<0°C) state.

Daily mean equatorial temperatures on Mars are close to 215 K. Surface geomorphic evidence of the flow of liquids, weathering minerals indicative of liquid/rock interactions, and the enrichment of heavy isotopes of several atmospheric species have led to suggestions that early Mars was significantly warmer, with temperatures possibly remaining above 273 K for extended periods of time (*1*). On the basis of crater counting statistics, the colder, drier conditions are thought to have emerged at ~3.7 billion years ago (Ga), with large (~10^8 to 10^9 years) uncertainties (*2*). The growing geochemical and petrographic data set for martian meteorites (*3*) provides an opportunity to constrain the martian paleoclimate using multiple independent samples. We used noble gas thermochronometry of meteorites as an indicator of the evolution of surface temperatures on Mars.

K/Ar and $^{40}Ar/^{39}Ar$ dating studies have been conducted on all seven known nakhlites (*4*) and on martian meteorite ALH84001 (*5*, *6*). Fifteen K/Ar analyses on the nakhlites all give ages of ~1.3 Ga, which are nearly identical to crystallization ages specified by the Rb/Sr, U/Pb, and Sm/Nd chronometers (*7*) and much older than the 11 million years ago (Ma) age of ejection from Mars, as specified by cosmic ray exposure dating (*8*, *9*). (U-Th)/He dating of the nahklites meteorites Nakhla, Lafayette, and MIL03346 (*10*, *11*) has measured similarly ancient (~0.8 to 1.2 Ga) ages. The coincidence of the K/Ar and (U-Th)/He ages with the other chronometers suggests that the nakhlites have experienced no major heating since they formed. Similarly, the ancient 4 Ga $^{40}Ar/^{39}Ar$ age (*6*) and 4 Ga U/Pb apatite age (*12*) for ALH84001 suggests that this meteorite, which has Rb/Sr and Sm/Nd crystallization ages of 4.5 Ga and a cosmic ray exposure age of 15 Ma (*13*), has not experienced any major heating since 4 Ga. This is generally consistent with (U-Th)/He dating of ALH84001 phosphate, which gives a wide range of ages between 0.1 and 3.5 Ga (*14*). Like the nakhlites, the $^{40}Ar/^{39}Ar$ age of Chassigny is ~1.3 Ga and is close to its Sm/Nd and Rb/Sr crystallization ages (*6*, *13*). $^{40}Ar/^{39}Ar$ ages for most shergottites are ambiguous because of significant abundances of trapped Ar (*6*, *13*).

Using whole-rock ^{39}Ar release data of Swindle and Olson (*15*) and following the methods of (*5*, *16*), we estimated the temperature dependence of the Ar diffusion coefficient $D(T)$ through the feldspar in Nakhla and Lafayette, assuming a spherical diffusion domain geometry (*17*). We first considered Swindle and Olson's Nakhla subsample 1. We assumed that the colinearity observed for the first ~80% of the released ^{39}Ar (Fig. 1) indicates that the diffusion of Ar in Nakhla is thermally activated over this range. We also assumed that the presence of distinct arrays clearly separated by breaks in slope (Fig. 1) indicates that multiple diffusion domains are present. From this, we identified three (or possibly even four) primary arrays from the ^{39}Ar data and adopted the interpretation of (*15*) that the first three domains [the low-retentivity domain (LRD) and the one or two high-retentivity domains, which we will refer to as HRD and HHRD] likely represent iddingsite (LRD) and predominantly potassium feldspar admixed with plagioclase (HRD and HHRD). The final array, composed of the final ~20% of gas released, appears to be from a phase (probably clinopyroxene) implanted with recoiled ^{39}Ar (*15*, *18*).

We characterized the spatial distribution of radiogenic ^{40}Ar ($^{40}Ar^*$) and the Ar diffusion kinetics in the HRD alone. The HRD corresponds to the ~1.3 Ga $^{40}Ar/^{39}Ar$ plateau age identified in (*15*). We calculated a diffusion domain model by assuming that the neutron-induced ^{39}Ar distributions were initially uniform within two distinct domains. Gas was not permitted to exchange between the domains. We derived the following diffusion parameters for the two-domain (LRD and HRD only) model for the HRD of Nakhla: activation energy E_a = 117 ± 5.4 kJ mol^{-1} and $\ln(D_o/a^2)$ = 5.7 ± 0.9 $\ln(s^{-1})$ for diffusivity at infinite temperature D_o and diffusive length scale a. These are in good agreement with diffusion parameters estimated for terrestrial potassium feldspars (*19*). Nearly identical results were obtained for the nakhlite Lafayette and another Nakhla subsample (fig. S1, A and B). Similar [within a factor of ~1.2 and ~2.4 for E_a and $\ln(D_o/a^2)$, respectively] values for the HRD were also obtained for a subset one-domain (HRD only) regression (*20*) and a three-domain (LRD, HRD, and HHRD) model, indicating that the inferred diffusion kinetics are not strongly sensitive to the form of the domain modeling (*21*).

In the following calculations, we assume that this Arrhenius relation and corresponding diffusive length scale a have held for the nakhlites' HRD since 1.3 Ga (*22*). The model

[1]Division of Geological and Planetary Sciences, California Institute of Technology, 100-23, Pasadena, CA 91125, USA. [2]Department of Earth, Atmospheric, and Planetary Sciences, Massachusetts Institute of Technology, 54-724, Cambridge, MA 02139, USA.

*Present address: Berkeley Geochronology Center, 2455 Ridge Road, Berkeley, CA 94709, USA
†To whom correspondence should be addressed. E-mail: bpweiss@mit.edu

LRD diffusion kinetics predict essentially no ^{40}Ar* retention over geologic time, which is consistent with the zero age ^{40}Ar/^{39}Ar in the first ~3% of extracted ^{39}Ar observed by (*15*). With the two-domain model (Fig. 1) and a numerical solution to the radiogenic production/diffusion equation described by (*5*, *23*) using a pre-atmospheric meteorite radius of 0.2 m (*8*), we simulated the expected ^{40}Ar* distributions within the sample after various thermal perturbations. The model ^{40}Ar* distributions were calculated for the HRD and then passed through a simulated degassing experiment to produce a set of ^{40}Ar* release fractions (Fig. 2).

Our calculations demonstrate that only ~1% of the ingrown ^{40}Ar* has been diffusively lost from the HRD of Nakhla and Lafayette since 1.3 Ga. From a similar analysis using the Ar release data of Bogard and Garrison (*6*), we confirm our conclusion (*5*) that less than 8% of the ingrown ^{40}Ar* has been diffusively lost from the HRD of ALH84001 since 4 Ga (figs. S1C and S2C).

Solving for a sample's continuous thermal history from an observed radiometric age and an inferred spatial distribution of the daughter product is an ill-posed problem: A family of thermal limits can be uniquely constrained, although a single solution does not generally exist (*19*). For instance, let us suppose that the nakhlites were heated to some peak temperature during ejection from Mars at 11 Ma. If we assume that the meteorites cooled diffusively and degassed ^{40}Ar* diffusively solely during this ejection event, then following the methods of (*5*), we find that the central temperatures of these meteorites could not have exceeded ~350°C for even short periods of time (no more than a few hours) (Fig. 2). This is a conservative upper limit, because we assume (i) that the diffusion domains are spherical and that during the other 1.3 billion years of history (ii) there was no other diffusive loss of ^{40}Ar* and (iii) no loss of ^{40}Ar* caused by nonthermal mechanisms (such as weathering or shock). These results are consistent with petrographic constraints, which suggest that the nakhlites have been shocked only to peak pressures of 10 to 20 GPa and peak temperatures of –50° to 100°C, respectively [following (*24*, *25*) and using ambient martian surface temperatures between –120° and 0°C]. Given the petrographic similarities linking the nakhlites, it is likely that the conclusions drawn from Nakhla and Lafayette extend to the five other known meteorites in this class.

Because the magnetization of the nakhlites is thought to be dominated by titanomagnetite with a Curie point of ~500° to 550°C (*26*), much of the magnetization measured in the nakhlites is likely to have been a thermoremanence that originated on Mars at 1.3 Ga. However, this remanence is likely to have been modified by shock (*27*).

Our results are consistent with the observed low shock state of nakhlites (*24*, *25*), which implies that they were not heat-sterilized (that is, they were cooler than ~100°C) during ejection from Mars and transfer to Earth. Although ALH84001 also is thought to have experienced only mild heating during its transfer to Earth (*5*, *28*), the case for the nakhlites is stronger because of their substantially lower shock state (*29*). This illustrates the efficiency of mechanisms for ejecting weakly shocked rocks from Mars (*24*, *30*) and underscores the possibility that the terrestrial planets have not been biologically isolated from one another.

Finally, these results highlight the difference in thermal histories between Mars and Earth. The small amounts of ^{40}Ar* degassing observed for the nakhlites and particularly for ALH84001 require that they must have been at low temperatures for nearly their entire histories. Linearly extrapolating the HRD Arrhenius relations (Fig. 1 and fig. S1) to low temperatures, we find that during the past 1.3 billion years, the three nakhlites could not have been at a constant temperature exceeding –8° to –49°C, depending on which Arrhenius model for the HRD is used (Fig. 3A and fig. S3A). A constant temperature of no more than –2° to –43°C lasting for 200 million

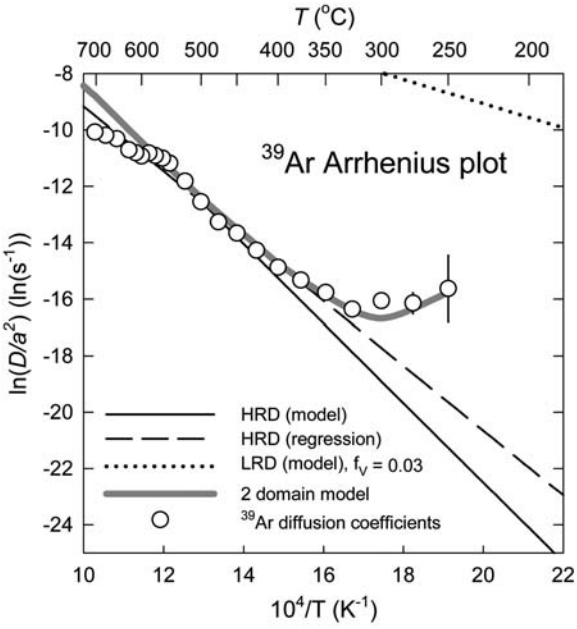

Fig. 1. Diffusivity as a function of temperature (Arrhenius plot) for martian meteorite Nakhla (subsample 1) inferred from ^{39}Ar release data of Swindle and Olson (*15*). Circles are the diffusion coefficients as calculated following (*16*). The bold gray curve shows the best-fit two-domain model, which contains a volume fraction f_v of 3% LRD mixed with 97% HRD. The solid and dotted black lines show model $D(T)/a^2$ for the HRD and LRD, respectively. The dashed black line shows the one-domain model, given by the linear regression fit only to the subset HRD array [it includes the 375° to 675°C steps (*20*)]. Error bars (specified by a vertical line through each point) are smaller than the size of the circle for all but the two lowest temperature steps. Similar results are obtained for both a second Nakhla subsample and for Lafayette (fig. S1).

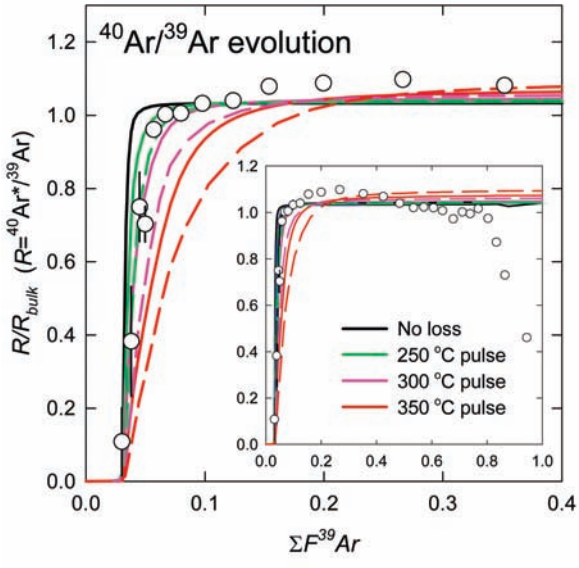

Fig. 2. Measured and modeled ^{40}Ar*/^{39}Ar ratio evolution spectra for martian meteorite Nakhla (subsample 1). These spectra were calculated using the two-domain model in Fig. 1 for various assumed diffusively cooling thermal pulses experienced by the HRD. Following (*19*), we found that it takes several hours for the meteorites to cool to ambient temperatures. The LRD was assumed to contain no radiogenic Ar (^{40}Ar*), and the spatial distribution of ^{40}Ar* within the HRD was assumed to be uniform before ejection. Shown are the calculated ^{40}Ar*/^{39}Ar ratios R (normalized to the bulk ratio R_{bulk}) plotted as a function of the cumulative ^{39}Ar release fraction ΣF^{39}Ar. Circles are the data of (*15*). Solid curves correspond to various peak temperature pulses during ejection from Mars at 11 Ma: black, no diffusive loss experienced by the HRD; green, 250°C; pink, 300°C; red, 350°C. Dashed curves are the same calculations using the one-domain model shown in Fig. 1. Error bars (specified by a vertical line through each point) are smaller than the size of the circle for all but the nine lowest temperature steps. Similar results are obtained for both a second Nakhla subsample and for Lafayette (fig. S2).

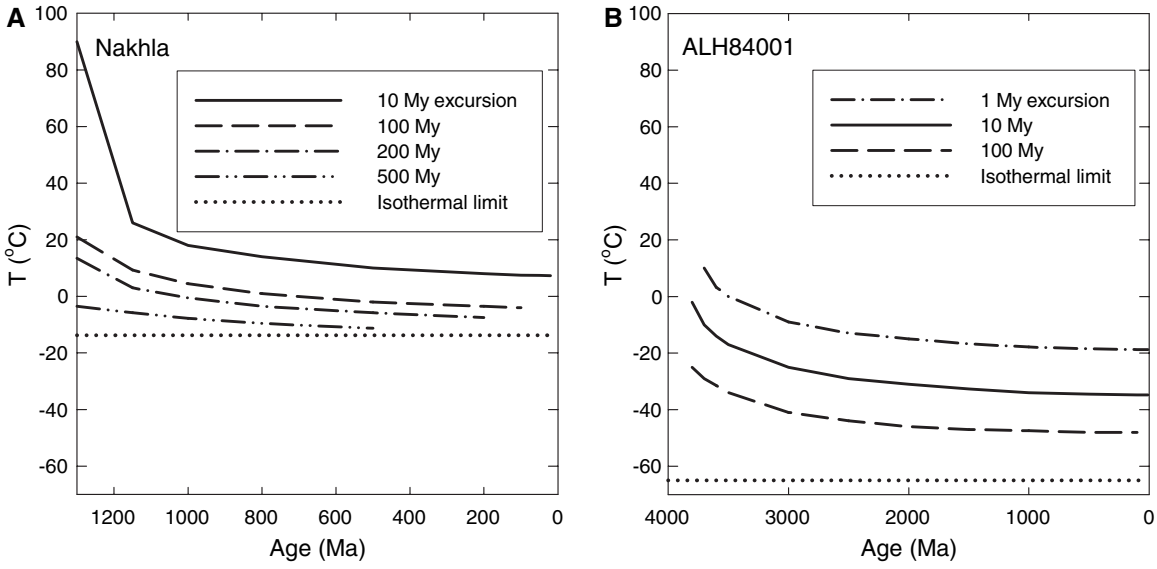

Fig. 3. Long-duration temperature limits for (**A**) Nakhla (subsample 1) and (**B**) ALH84001. Curves depict the maximum temperature that each meteorite could have experienced during a single assumed temperature excursion as a function of the time before the present (age) in martian history when the excursion begins. Each curve corresponds to a particular assumed duration for the excursion. The HRDs of the meteorites are assumed to experience no diffusive loss of ^{40}Ar* at all times other than during the temperature excursion. Each model is constrained to match the deficit gas fraction (the diffusively lost proportion of ^{40}Ar* relative to complete retention) observed in the HRD of each meteorite today (1 and 8% for Nakhla and ALH84001, respectively). These curves were calculated using the two-domain Arrhenius relations in Fig. 1. Figure S3 shows the sensitivity of these time/temperature constraints to the uncertainties in the diffusion kinetics.

years of the past 1 billion years of Nakhla's history is also required. This result is consistent with constraints derived from ALH84001, which suggest that since 4 Ga, it could not have been at a constant temperature exceeding –60° to –70°C, and since 3.5 Ga it could not have been warmer than –7° to +7°C for all but the briefest time period (1 million years) (Fig. 3B and fig. S3B). Given our assumptions, these are conservative upper limits. In all, four subsamples from three rocks taken from two martian meteorite classes with vastly different ages, petrographic textures, compositions, and argon diffusion kinetics give similar constraints on martian temperatures.

Our results may seem surprising given that Mars' obliquity and surface temperatures are thought to have regularly reached high values over the planet's entire history, with dominant frequencies of ~120,000 years and longer (*1*, *31*). However, because temperature changes at the martian surface will be attenuated at depth, deeply buried rocks may not sample these events (*1*, *32*). Although the burial depths of the martian meteorites are largely unknown, it is conceivable that ALH84001 was at more than 1 km depth for the past 4 billion years, whereas the nakhlites likely resided at depths of between a few meters to no more than a few hundred meters (*33*). Therefore, all of the meteorites subjected to the thermochronological calculations described here should not have been subject to diurnal or annual thermal variations. ALH84001 may not have sampled even the longest-period obliquity-induced thermal waves. However, the nakhlites formed at such shallow depths that they almost certainly experienced elevated temperatures associated with the full frequency range of obliquity changes since 1.3 Ga.

Our calculations imply that during the past 4 billion years, average temperatures within the top few kilometers of the martian crust were not significantly warmer than the present cold (subzero) conditions and therefore that pure liquid water was not likely to have been stable at the martian surface for extended periods of time. This is consistent with suggestions (*34*) that the secondary minerals only observed in these meteorites are the products of brief (less than a few days) interactions with liquid water.

References and Notes

1. M. Carr, *Water on Mars* (Oxford Univ. Press, Oxford, 1996).
2. W. K. Hartmann, G. Neukum, *Space Sci. Rev.* **96**, 165 (2001).
3. C. Meyer, *Mars Meteorite Compendium—2003* (NASA Johnson Space Center, Houston, TX, 2003), www-curator.jsc.nasa.gov/curator/antmet/mmc/mmc.htm.
4. Additional details about ^{40}Ar/^{39}Ar dating of nakhlites and our thermochronology methods are available as supporting material on *Science* Online.
5. B. P. Weiss, D. L. Shuster, S. T. Stewart, *Earth Planet. Sci. Lett.* **201**, 465 (2002).
6. D. D. Bogard, D. H. Garrison, *Meteorit. Planet. Sci.* **34**, 451 (1999).
7. H. Y. McSween, A. H. Treiman, in *Planetary Materials*, J. J. Papike, Ed. (Mineralogical Association of America, Washington, DC, 1998), pp. 6-1 to 6-53.
8. O. Eugster, H. Busemann, S. Lorenzetti, D. Terrebilini, *Meteorit. Planet. Sci.* **37**, 1345 (2002).
9. K. Marti, K. J. Mathew, *Antarct. Meteorite Res.* **17**, 117 (2004).
10. R. Ganapathy, E. Anders, *Geochim. Cosmochim. Acta* **33**, 775 (1969).
11. S. V. S. Murty, R. R. Mahajan, J. N. Goswami, N. Sinha, *Lunar Planet. Sci.* **XXXVI**, abstract 1280 (2005).
12. K. Terada, T. Monde, Y. Sano, *Meteorit. Planet. Sci.* **38**, 1697 (2003).
13. L. E. Nyquist *et al.*, *Space Sci. Rev.* **96**, 105 (2001).
14. K. Min, P. W. Reiners, *Lunar Planet. Sci.* **XXXVI**, abstract 2214 (2005).
15. T. D. Swindle, E. K. Olson, *Meteorit. Planet. Sci.* **39**, 755 (2004).
16. H. Fechtig, S. Kalbitzer, in *Potassium-Argon Dating*, O. A. Schaeffer, J. Zahringer, Eds. (Springer, Heidelberg, Germany, 1966), pp. 68–106.
17. The four highest temperature steps with ^{40}Ar/^{39}Ar clearly influenced by ^{39}Ar recoil were excluded from the total ^{39}Ar abundance used to calculate ^{39}Ar release fractions. Because these four steps were likely derived from a K-poor phase with higher Ar retentivity than the HRD of interest, they were excluded from the total so as not to bias the calculated diffusion coefficients for the lower-temperature extractions.
18. R. Burgess, G. Holland, V. Fernandes, G. Turner, *J. Conf. Abs.* **5**, 266 (2000).
19. I. McDougall, T. M. Harrison, *Geochronology and Thermochronology by the ^{40}Ar/^{39}Ar Method* (Oxford Univ. Press, New York, ed. 2, 1999).
20. In a sample with multiple and distinct diffusion domains, and for stepwise extractions that sequentially increase in temperature, linear regression through a subset array in a plot of $\ln(D/a^2)$ versus $1/T$ places lower bounds on the activation energy and $\ln(D_o/a^2)$ for the domain that dominates Ar release at those steps. Therefore, this one-domain model places maximum bounds on Ar diffusivity at low-temperature extrapolations. For this regression, the linear subset array was selected for steps between 375° and 675°C.
21. O. M. Lovera, M. Grove, T. M. Harrison, *Geochim. Cosmochim. Acta* **66**, 1237 (2002).
22. Specifically, we assume that the HRD argon diffusion kinetics measured in the laboratory between 250° and 700°C can be extrapolated to the (i) longer time scales, (ii) lower temperatures, and (iii) different pressures encountered in nature. We also assume that the characteristic diffusive length scale *a* of the HRD implied by Fig. 1 has not been modified since the initiation of ^{40}Ar* accumulation. Because the nakhlites were shock-fractured sometime after their formation (*25*), we are implicitly assuming that *a* is smaller than the characteristic distances between cracks and that the diffusion domains are not defined by the bulk geometry of the feldspar fragments.
23. D. L. Shuster, K. A. Farley, *Earth Planet. Sci. Lett.* **217**, 1 (2004).
24. N. Artemieva, B. Ivanov, *Icarus* **171**, 84 (2004).
25. J. Fritz, A. Greshake, D. Stoffler, *Lunar Planet. Sci.* **XXXIV**, abstract 1335 (2003).
26. D. W. Collinson, *Meteorit. Planet. Sci.* **32**, 803 (1997).
27. S. A. Gilder, M. LeGoff, J. C. Chervin, J. Peyronneau, *Geophys. Res. Lett.* **31**, L10612 (2004).
28. B. P. Weiss *et al.*, *Science* **290**, 791 (2000).
29. ALH84001 has been shocked to >40 GPa, but our thermochronological calculations indicate that this occurred at 4 Ga rather than during ejection (*5*). Although paleomagnetic analyses have been used to argue that ALH84001 was cooler than 40°C (*28*), it is

possible that the observed low-temperature paleomagnetic remanence was affected by viscous remagnetization. The thermal histories experienced by shergottites and chassignites are less well known because of the paucity of magnetic analyses and high-resolution $^{40}Ar/^{39}Ar$ age spectra free of trapped Ar for these rocks. (U-Th)/He dating of the shergottite Los Angeles (*35*) found that the meteorite was strongly heated (to probably at least several hundred degrees C) during ejection, but the peak temperature is not well constrained because the diffusivity of helium in Los Angeles merrillite is not currently known.

30. H. J. Melosh, *Nature* **363**, 498 (1993).
31. J. Laskar *et al.*, *Icarus* **170**, 343 (2004).
32. F. P. Fanale, J. R. Salvail, W. B. Banerdt, R. S. Saunders, *Icarus* **50**, 381 (1982).
33. Cosmic ray exposure data (*8*) imply that ALH84001 and most of the nakhlites must have been buried at least a few meters deep for nearly all of their histories. The nakhlites are thought to be cumulate rocks that originated in a shallow intrusion or lava flow. Analyses of iron and magnesium zoning in nakhlite olivines (*36*) suggest that Nakhla and Lafayette formed at depths of 3 to 10 m and >30 m, respectively. These estimates are consistent with but more restrictive than depth estimates inferred from studies of Theo's Flow, which are ultramafic lavas several hundred meters thick thought to be a terrestrial analog for the nakhlite source region (*37*, *38*). ALH84001 probably formed as a cumulate in a deep (several tens of kilometers) intrusion (*7*). However, given our thermal constraints, two observations suggest that it was later excavated to much shallower depths. First, the thermal gradient on Mars, although not well constrained, is thought to be ~10°C/km. Second, ALH84001 was strongly shocked at least twice (once before 4 Ga and then again at 4 Ga) (*5*, *7*, *39*) and then ejected from Mars without experiencing postshock temperatures greater than 350°C. This suggests that by the 15 Ma ejection event, it resided in the spall zone of the impactor. For a 10-km impactor, this would imply a burial depth of no more than a few kilometers (*40*).
34. J. C. Bridges *et al.*, *Space Sci. Rev.* **96**, 365 (2001).
35. K. Min, P. W. Reiners, S. Nicolescu, J. P. Greenwood, *Geology* **32**, 677 (2004).
36. T. Mikouchi, E. Koizumi, A. Monkawa, Y. Ueda, M. Miyamoto, *Antarct. Meteorite Res.* **16**, 34 (2003).
37. R. C. F. Lentz, G. J. Taylor, A. H. Treiman, *Meteorit. Planet. Sci.* **34**, 919 (1999).
38. A. H. Treiman, *Lunar Planet. Sci.* **XVIII**, 1022 (1987).
39. J. P. Greenwood, H. Y. McSween, *Meteorit. Planet. Sci.* **36**, 43 (2001).
40. H. J. Melosh, *Impact Cratering: A Geologic Process* (Oxford Univ. Press, Oxford, 1986).

41. We thank T. Swindle and D. Bogard for generously sharing their Ar data with us and for helpful discussions, along with T. Grove, A. Maloof, and J. Eiler. B.P.W. is supported by the NASA Mars Fundamental Research and NSF Geophysics programs.

Supporting Online Material

www.sciencemag.org/cgi/content/full/309/5734/594/DC1
SOM Text
Figs. S1 to S3
References

4 April 2005; accepted 7 June 2005
10.1126/science.1113077

Genomic Sequencing of Pleistocene Cave Bears

James P. Noonan,[1,2] Michael Hofreiter,[3] Doug Smith,[1] James R. Priest,[2] Nadin Rohland,[3] Gernot Rabeder,[4] Johannes Krause,[3] J. Chris Detter,[1,5] Svante Pääbo,[3] Edward M. Rubin[1,2]*

Despite the greater information content of genomic DNA, ancient DNA studies have largely been limited to the amplification of mitochondrial sequences. Here we describe metagenomic libraries constructed with unamplified DNA extracted from skeletal remains of two 40,000-year-old extinct cave bears. Analysis of ~1 megabase of sequence from each library showed that despite significant microbial contamination, 5.8 and 1.1% of clones contained cave bear inserts, yielding 26,861 base pairs of cave bear genome sequence. Comparison of cave bear and modern bear sequences revealed the evolutionary relationship of these lineages. The metagenomic approach used here establishes the feasibility of ancient DNA genome sequencing programs.

Genomic DNA sequences from extinct species can help reveal the process of molecular evolution that produced modern genomes. However, the recovery of ancient DNA is technologically challenging, because the molecules are degraded and mixed with microbial contaminants, and individual nucleotides are often chemically damaged (*1*, *2*). In addition, ancient remains are invariably contaminated with modern DNA, which amplifies efficiently compared with ancient DNA, and therefore inhibits the detection of ancient genomic sequences (*1*, *2*). These factors have limited most previous studies of ancient DNA sequences to polymerase chain reaction (PCR) amplification of mitochondrial DNA (*3*–*8*). In exceptional cases, small amounts of single-copy nuclear DNA have been recovered from ancient remains less than 20,000 years old obtained from permafrost or desert environments, which are well suited to preserving ancient DNA (*9*–*12*). However, the remains of most ancient animals, including hominids, have not been found in such environments.

To circumvent these challenges, we developed an amplification-independent direct-cloning approach to constructing metagenomic libraries from ancient DNA (Fig. 1). Ancient remains are obtained from natural environments in which they have resided for thousands of years, and their extracted DNA is a mixture of genome fragments from the ancient organism and sequences derived from other organisms in the environment. A metagenomic approach, in which all genome sequences in an environment are anonymously cloned into a single library, may therefore be a powerful alternative to the targeted PCR approaches that have been used to recover ancient DNA molecules. We chose to explore this strategy with the extinct cave bear instead of an extinct hominid, to unambiguously assess the issue of modern human contamination (*1*, *2*). In addition, because of the close evolutionary relationship of bears and dogs, cave bear sequences in these libraries can be identified and classified by comparing them to the available annotated dog genome. The phylogenetic relationship of cave bears and modern bear species has also been inferred from mitochondrial sequences, providing the opportunity to compare the phylogenetic information content of cave bear mitochondrial and genomic DNA (*13*).

We extracted DNA from a cave bear tooth recovered from Ochsenhalt Cave, Austria, and a cave bear bone from Gamssulzen Cave, Austria, dated at 42,290 (error +970/–870) and 44,160 (+1400/–1190) years before the present, respectively, by accelerator mass spectrometry radiocarbon dating (table S1). We used these ancient DNA molecules to construct two metagenomic libraries, designated CB1 and CB2 (Fig. 1) (*14*). These libraries were constructed in a laboratory into which modern carnivore DNA has never been introduced. Ancient DNA molecules were blunt end–repaired before ligation but were otherwise neither enzymatically treated nor amplified. We sequenced 9035 clones [1.06 megabases (Mb)] from library CB1 and 4992 clones (1.03 Mb) from library CB2. The average insert sizes for each library were 118 base pairs (bp) and 207 bp, respectively.

We compared each insert in these libraries to GenBank nucleotide, protein, and environmental sequences, and the July 2004 dog whole genome shotgun assembly, by using Basic Local Alignment Search Tool (BLAST) software with an expect value cutoff of 0.001 and a minimum hit size of 30 bp (*14*–*16*). 1.1% of clones in library CB1 (Fig. 2A) and 5.8% of clones in library CB2 (Fig. 2B) had significant hits to dog genome or modern bear sequences. Our direct-cloning approach produces chimeric inserts, so we defined as candidate cave bear

[1]United States Department of Energy Joint Genome Institute, Walnut Creek, CA 94598, USA. [2]Genomics Division, Lawrence Berkeley National Laboratory, Berkeley, CA 94720, USA. [3]Max Planck Institute for Evolutionary Anthropology, Leipzig, D-04103, Germany. [4]Institute of Paleontology, University of Vienna, Vienna, A-1010 Austria. [5]Biosciences Directorate, Lawrence Livermore National Laboratory, Livermore, CA 94550, USA.

*To whom correspondence should be addressed. E-mail: emrubin@lbl.gov

Supplementary Information for:

Shuster, D. L. and B. P. Weiss (2005) Martian Surface Paleotemperatures from Thermochronology of Meteorites, *Science*

At least fifteen K/Ar and $^{40}Ar/^{39}Ar$ dating studies targeting both whole rock and mineral separates have been conducted on the nakhlites (*1-16*). This study relies on the recently published $^{40}Ar/^{39}Ar$ study of Swindle and Olson (*13*) and Bogard and Garrison (*17*), which had many heating steps, enabling us to characterize the spatial distribution of Ar in the meteorites with high spatial resolution.

Fig. S1. Diffusivity as a function of temperature (Arrhenius plot) for (**A**) Nakhla (subsample 2) (**B**) Lafayette, and (**C**) ALH84001 inferred from the ^{39}Ar release data of Swindle and Olson (*13*) and Bogard and Garrison (*17*). Circles are the diffusion coefficients as calculated following (*18*). Red curves: best-fit two-domain model. Solid and dotted black lines: model $D(T)/a^2$ for the high-retentivity domains (HRD) and low-retentivity domain (LRD), respectively. Dashed black lines: one-domain models, given by the linear regression fit only to the subset HRD arrays (temperature steps 375° to 675 °C). Error bars (specified by vertical line through each point) are smaller than the size of the circles for all but the lowest three temperature steps.

Fig. S2. Measured and modeled $^{40}Ar^*/^{39}Ar$ ratio evolution spectra for (**A**) Nakhla (subsample 2) (**B**) Lafayette and (**C**) ALH84001. These spectra were calculated using the two-domain models shown in Fig. S1 for various assumed diffusively-cooling thermal pulses experienced by the high-retentivity domain (HRD). Shown are the calculated $^{40}Ar^*/^{39}Ar$ ratios, R (normalized to the bulk ratio, R_{bulk}) plotted as a function of the cumulative ^{39}Ar release fraction $\Sigma F^{39}Ar$. Circles are the data of (*13*) (for Nakhla and Lafayette) and (*17*) (for ALH84001). Solid curves correspond to various temperature pulses during ejection from Mars which occurred at 11 Ma and 15 Ma for the nakhlites and ALH84001, respectively: black = no diffusive loss experienced by the HRD, green = 250 °C, pink = 300 °C, red = 350 °C, dark green = 400 °C, dark red = 450 °C. For the nakhlites, the low retentivity domain (LRD) was assumed to contain no $^{40}Ar^*$, while for

ALH84001, the LRD was assumed to be completely full of $^{40}Ar^*$ prior to the thermal pulse. Error bars (specified by vertical line through each point) are smaller than the size of the circles for all but the lowest 8 temperature steps.

Fig. S3. Estimated uncertainties for the time-temperature limits in Fig. 3 in the main text for (**A**) Nakhla and (**B**) ALH84001. For Nakhla, the HRD diffusion kinetics differ depending on whether one uses a one-, two- or three-domain model. The differences in the diffusion kinetics between these models are larger than the formal regression errors for the kinetics in the one-domain model. The opposite is true for ALH84001, for which the best-fit HRD diffusion kinetics for the one- and two-domain model are the same. Therefore, for Nakhla we estimated the uncertainty in the time-temperature limits using the range in diffusion kinetics implied by the different domain models, while for ALH84001 we estimated the uncertainty using the formal regression errors of the one-domain model. The range of values for a given temperature excursion duration are shaded so as to provide a sense of the uncertainty envelope around the favored two-domain models shown in Fig. 3. My, millions of years. **(A)** Each triplet of curves depicts the maximum constant temperature that the meteorite could have experienced as a function of the time in history at which the temperature excursion is assumed to occur, calculated using the one, two, and three-domain diffusion models. Each triplet corresponds to a particular assumed duration for the temperature excursion. The HRD of the meteorites are assumed to experience no diffusive loss at all times other than during the temperature excursion. The one-domain models slightly overestimate the diffusivity and so place a rough lower bound on our estimate of the maximum temperature. The two- and three-domain models give roughly similar estimates of the maximum temperature, with the latter models giving slightly higher values. We favor the two-domain models because they fit the data much better than the one-domain models while also requiring a smaller number of tunable parameters than the three-domain models (5 parameters instead of 8). **(B)** The triplet of curves for ALH84001 is calculated from the maximum range in diffusion kinetics implied by the formal regression errors at the 95% confidence interval.

References

1. H. Stauffer, *J. Geophys. Res.* **67**, 2023 (1962).
2. R. Ganapathy, E. Anders, *Geochim. Cosmochim. Acta* **33**, 775 (1969).
3. F. A. Podosek, *Earth Planet. Sci. Lett.* **19**, 135 (1973).
4. F. A. Podosek, J. C. Huneke, *Geochim. Cosmochim. Acta* **37**, 667 (1973).
5. D. D. Bogard, L. Husain, *Geophys. Res. Lett.* **4**, 69 (1977).
6. U. Ott, *Geochim. Cosmochim. Acta* **52**, 1937 (1988).
7. J. D. Gilmour, R. Burgess, J. A. Whitby, G. Turner, *Lunar Planet. Sci. XXIX*, abstract #1788 (1998).
8. R. Burgess, G. Holand, V. Fernandes, G. Turner, *J. Conf. Abs.* **5**, 266 (2000).
9. T. D. Swindle *et al.*, *Meteorit. Planet. Sci.* **35**, 107 (2000).
10. K. J. Mathew, B. Marty, K. Marti, L. Zimmermann, *Earth Planet. Sci. Lett.* **214**, 27 (2003).
11. R. Okazaki, K. Nagao, N. Imae, H. Kojima, *Antarct. Meteorite Res.* **16**, 58 (2003).
12. K. Marti, K. J. Mathew, *Antarct. Meteorite Res.* **17**, 117 (2004).
13. T. D. Swindle, E. K. Olson, *Meteorit. Planet. Sci.* **39**, 755 (2004).
14. S. V. S. Murty, R. R. Mahajan, J. N. Goswami, N. Sinha, *Lunar Planet. Sci. XXXVI*, abstract #1280 (2005).
15. D. H. Garrison, D. D. Bogard, *Lunar Planet. Sci. XXXVI*, abstract #1137 (2005).
16. L. E. Nyquist *et al.*, *Space Sci. Rev.* **96**, 105 (2001).
17. D. D. Bogard, D. H. Garrison, *Meteorit. Planet. Sci.* **34**, 451 (1999).
18. H. Fechtig, S. Kalbitzer, in *Potassium-Argon Dating* O. A. Schaeffer, J. Zahringer, Eds. (Springer, Heidelberg, 1966) pp. 68-106.

Shuster and Weiss (2005)
Figure S1

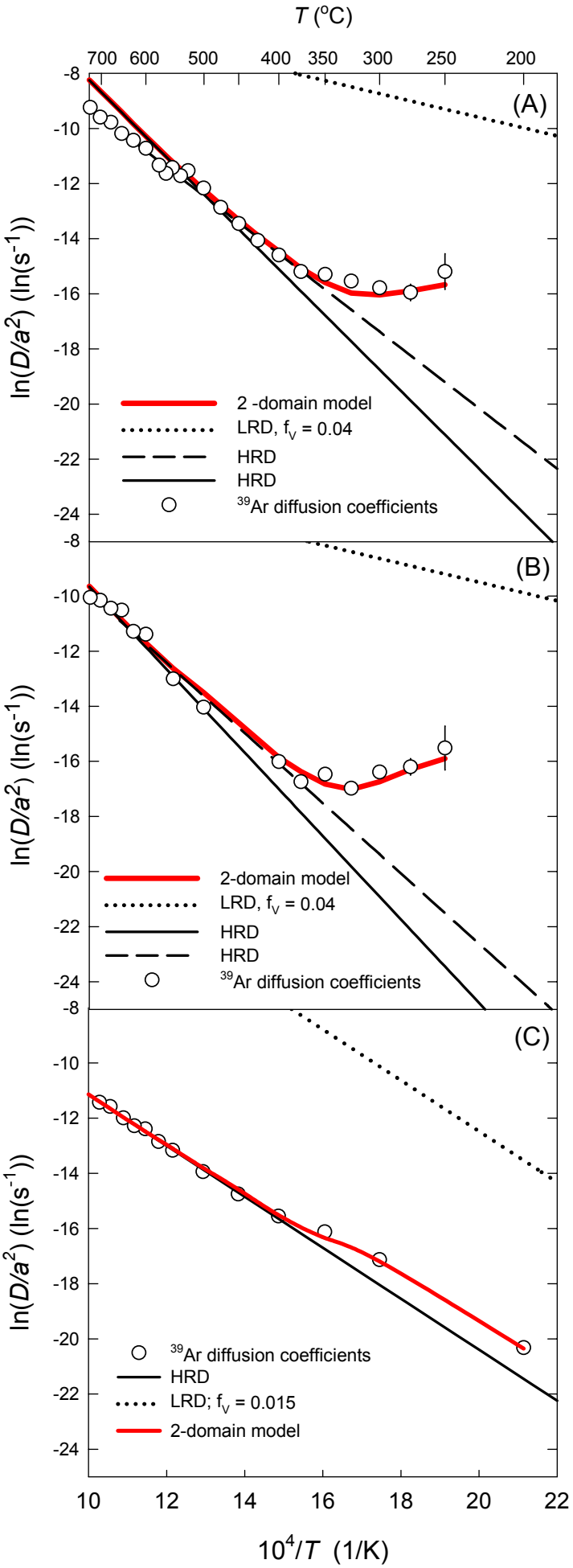

Shuster and Weiss (2005)
Figure S2

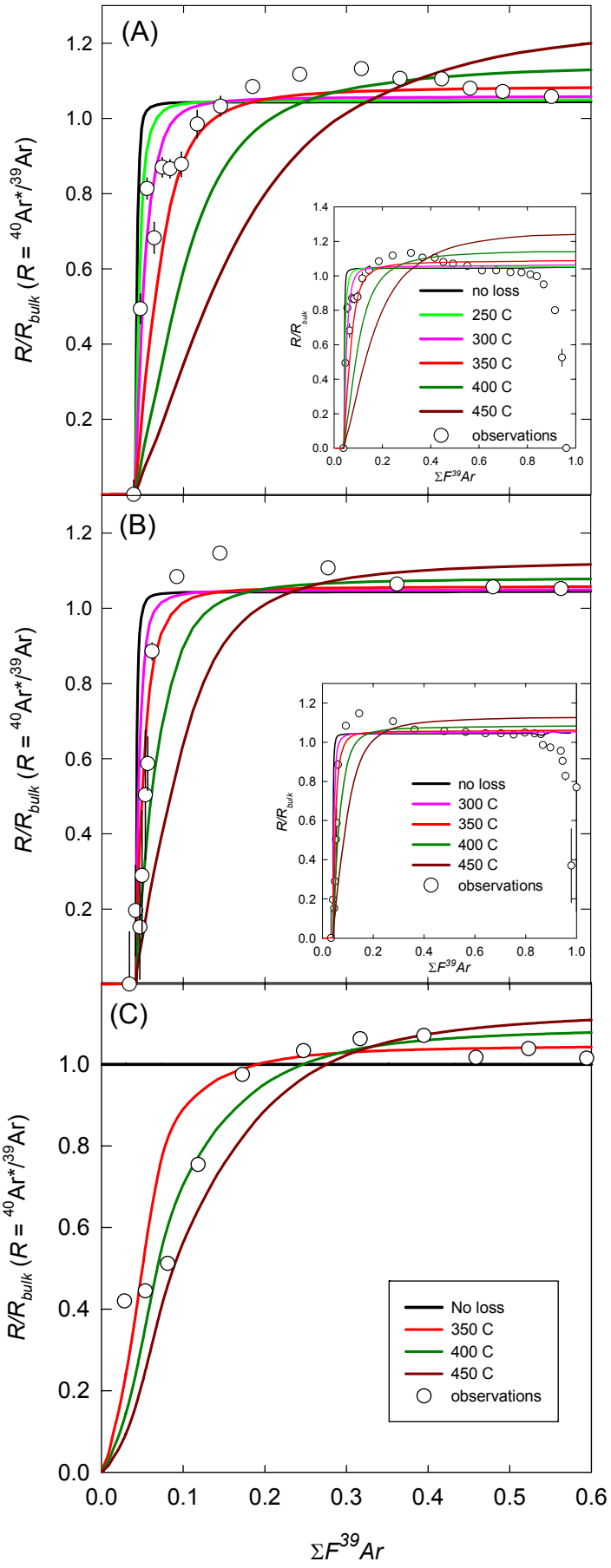

Shuster and Weiss (2005)
Figure S3

(A) Nakhla

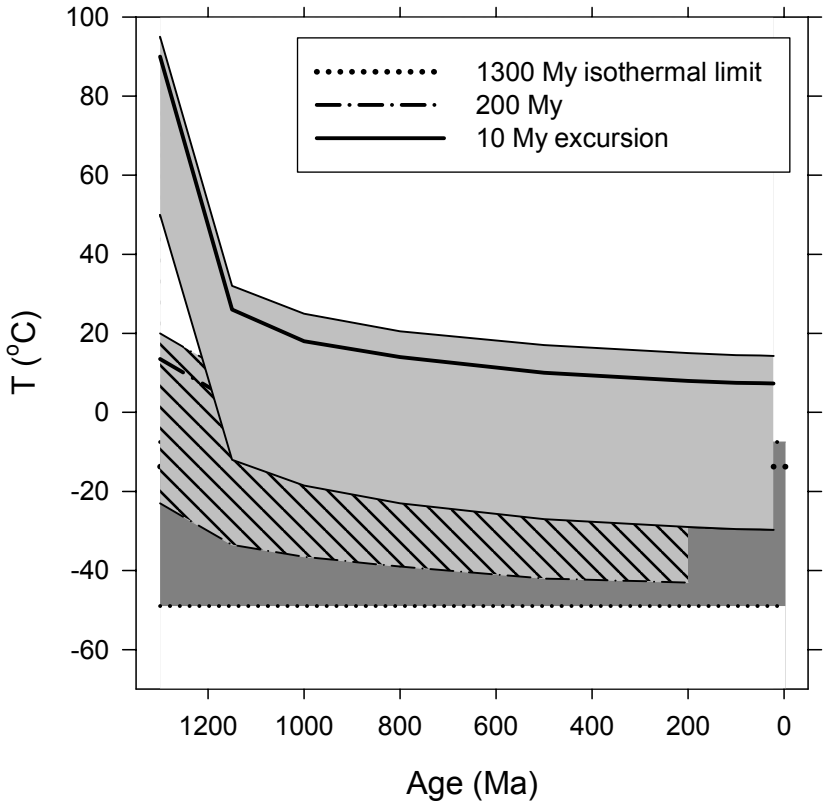

(B) ALH84001